J Mol Model (2013) 19:859–870
DOI 10.1007/s00894-012-1614-x

ORIGINAL PAPER

Adsorption of CO molecule on AlN nanotubes by parallel electric field

Ali Ahmadi Peyghan · Mohammad T. Baei · Saeedeh Hashemian · Parviz Torabi

Received: 25 June 2012 / Accepted: 27 September 2012 / Published online: 17 October 2012

Abstract The behavior of the carbon monoxide (CO) adsorbed on the external surface of H-capped (6,0) zigzag single-walled aluminum nitride nanotube (AlNNT) was studied using parallel and transverse electric field (strengths 0–140×10^{-4} a.u.) and density functional calculations. The calculated adsorption energies of the CO/AlNNT complex increased with increasing parallel electric field intensity, whereas the adsorption energy values at the applied transverse electric field show a significant reverse trend. The calculated adsorption energies of the complex at the applied parallel electric field strengths increased gradually from −0.42 eV at zero field strength to −0.80 eV at a field strength of 140×10^{-4} a.u. The considerable changes in the adsorption energies and energy gap values generated by the applied parallel electric field strengths show the high sensitivity of the electronic properties of AlNNT towards the adsorption of CO on its surface. Analysis of structural parameters indicates that the nanotube is resistant to external electric field strengths. The dipole moment variations in the complex show a significant change in the presence of parallel and transverse electric fields, which results in much stronger interactions at higher electric field strengths. Additionally, the natural bond orbital charges, quantum molecular descriptors, and molecular orbital energies of the complex show that the nanotube can absorb CO molecule in its pristine form at a high applied parallel electric field, and that the nanotube can be used as a CO storage medium.

Keywords Sensor · Aluminum nitride nanotube · Adsorption · CO storage · Dipole moment

Introduction

In recent decades, investigations into new semiconducting materials for carbon monoxide (CO) sensor application have increased [1]. Carbon monoxide is a harmful gas for the human body and is also a main cause of air pollution. Therefore, many investigations have been undertaken to develop rapid, simple, and sensitive methods for detecting CO [2–4]. CO molecules affect the electronic transport properties of nanotubes via physisorption or chemisorption. However, several pure nanotubes cannot be used for detection of CO molecules because CO cannot be adsorbed completely on their surfaces. Therefore, experimental and theoretical investigations have focused on improving the sensing performance of such pristine tubes toward various gas molecules by doping or functionalizing [2–4].

Aluminum nitride nanotubes (AlNNTs) are inorganic analog carbon nanotubes (CNTs). They are isoelectronic with CNTs, and have been synthesized successfully by different research groups [5–7]. Because of their high temperature stability, large energy gap, thermal conductivity, and low thermal expansion [8], AlNNTs and aluminum

Electronic supplementary material The online version of this article (doi:10.1007/s00894-012-1614-x) contains supplementary material, which is available to authorized users.

A. A. Peyghan
Young Researchers Club, Islamshahr Branch,
Islamic Azad University,
Tehran, Iran

M. T. Baei (✉)
Department of Chemistry, Azadshahr Branch,
Islamic Azad University,
Azadshahr, Golestan, Iran
e-mail: Baei52@yahoo.com

S. Hashemian
Department of Chemistry, Yazd Branch, Islamic Azad University,
Yazd, Iran

P. Torabi
Department of Chemistry, Mahshahr Branch,
Islamic Azad University,
Mahshahr, Iran

nitride nanomaterials are used widely in technological applications, mainly in micro and optoelectronics such as laser diodes and solar-blind ultraviolet photodetectors and semiconductors [8]. Unlike CNTs, AlNNTs exhibit electronic properties and semiconductor behavior independent of length, tubular diameter and chirality. Tuning the electronic structures of the semiconducting AlNNTs for specific application is important in building specific electronic and mechanical devices.

Improving the sensing performance of the pristine nanotubes and nano sheets by manipulating their structure is too expensive; thus, the search for high sensitive pristine nanotubes generates high scientific interest. The electric field effect is one of the best techniques with which to study the electronic structure properties of nanotubes and adsorption of gaseous molecules on tube surfaces. In recent years, several studies on the computational calculation of field effects on the electronic and structural properties of nanotubes have been published [9–11]. However, to our knowledge, no experiments and theoretical investigation have been reported for CO adsorption on AlNNT surfaces under electric field effects.

Investigation of the chemisorption of CO on AlNNT surfaces is important in the field of CO storage and CO sensors. In this work, density functional calculations were used to study adsorption of CO on the outer surface of (6,0) zigzag AlNNT. The structural and electronic properties, charge density distributions, electric dipole moment variations, and molecular orbital energy analysis of the complex were studied. Also, the quantum molecular descriptors [12, 13] including electronic chemical potential (μ), global hardness (η), electrophilicity index (ω) [14], energy gap, global softness (S), and electronegativity (χ) of the complex under the influence of both parallel and perpendicular static external electric fields were investigated.

The results of our calculations indicate that CO adsorption on AlNNT is very sensitive to the strength of the electric field applied to the AlNNT surface, and that adsorption can be enhanced simply by controlling the direction of the electric field. In addition, the calculations indicated that CO adsorption on AlNNT under the electric field effect had a significant influence in comparison with CO adsorption by doping and functionalization methods [2–4]. The results indicate that the electric field effect on the AlNNT is a suitable method for CO adsorption, production of CO sensors, and other applications.

Computational methods

In the present work, the adsorption behaviors of the CO molecule on the (6,0) zigzag AlNNT were studied by means of density functional theory (DFT) calculations, in which the ends of the nanotube were saturated with hydrogen atoms. Due to the absence of periodic boundary conditions in molecular calculations, it was necessary to saturate the dangling Al and N bonds with H atoms. The influence of CO adsorption on the structural and electronic properties of the (6, 0) zigzag AlNNT was investigated. The hydrogenated model of the CO/AlNNT complex consists of 74 ($Al_{30}N_{30}H_{12}CO$) atoms. In the first step, all the atomic geometrical parameters of the structure were allowed to relax in the optimization at the DFT level of B3LYP exchange functional and 6-31G* standard basis set. The adsorption energy (E_{ads}) of the CO/AlNNT complex was calculated as follows:

$$E_{ads} = \left[E_{\mathrm{CO/AlNNT}}\right] - \left[E_{\mathrm{AlNNT}} + E_{\mathrm{CO}}\right] + E_{BSSE} \quad (1)$$

Where $E_{\mathrm{CO/AlNNT}}$ was obtained from full optimization of the CO/AlNNT complex, E_{AlNNT} and E_{CO} are the energy of the optimized AlNNT and CO structures, and E_{BSSE} is the BSSE corrected for the all interaction energies [15]. Negative or positive value for E_{ads} is referred to exothermic or endothermic processes, respectively. The influence of the static external electric field on the adsorption, structural, and electronic properties of the complex was then studied. The static external electric field applied separately at the positive X- and positive Y-directions, which are parallel and perpendicular to X and Y plane, respectively. The numerical values of static electric field strengths in the X and Y directions on the CO/AlNNT complex are 35×10^{-4}, 70×10^{-4}, 100×10^{-4}, and 140×10^{-4}a.u. (1 a.u.=5.14224×10^{11} V/m) [16]. The structural and electronic properties were based on Al–N bond lengths, bond angles, length of tube, tip diameters, dipole moment variations (D_{M}), energy gaps, energies, atomic charges, molecular orbital energies, adsorption energy, density of states, quantum molecular descriptors for the complex in above electric fields with X and Y orientations. For the optimized complex, the quantum molecular descriptors [12, 13] including electronic chemical potential (μ), global hardness (η), electrophilicity index (ω) [14], energy gap, global softness (S), and electronegativity (χ), was calculated as follows:

$$[\mu = -\chi = -(I + A)/2], [\eta = (I - A)/2], [\omega = \mu^2/2\eta], \text{and}[\mathrm{S} = 1/2\eta] \quad (2)$$

Where I ($- E_{\mathrm{HOMO}}$) is the first vertical ionization energy and A ($-E_{\mathrm{LUMO}}$) the electron affinity of the molecule. The electrophilicity index is a measure of the electrophilic power of a molecule. When two molecules react with each other, one molecule behaves as a nucleophile, whereas the other acts as an electrophile. A higher electrophilicity index shows higher electrophilicity of a molecule. The quantum molecular descriptors were compared in the static external electric fields. All calculations were carried out using the GAMESS suite of programs [17].

Results and discussion

CO adsorption on the (6,0) zigzag AlNNT

Four possible sites (i.e., the center site, above the hexagon, the Al and N sites above the aluminum and nitrogen atoms, and the Z site above the *zigzag* and axial Al–N bond) with two orientation (C-down and O-down) were considered (Fig. 1a, b). The notation C-down and O-down denotes a CO molecule oriented perpendicular to the surface via C and O atoms.

The interaction of CO with nanotube outer walls was examined. In the first step, the structures were allowed to relax by all atomic geometrical parameters in the optimization at the DFT level of B3LYP exchange-functional and 6-31G* standard basis set. Having done structural optimizations, it was found that CO adsorption on center, nitrogen, and Z sites of the nanotube are energetically unstable and was collapsed to the aluminum site, which is energetically favorable. The adsorption energies (E_{ads}) of CO (C-down and O-down) with the equilibrium distances ($R_{Al\text{-}C}$ and $R_{Al\text{-}O}$) at the aluminum site on the zigzag configuration of (6,0) AlNNT are summarized in Fig. 1a, b. For the states, the adsorption energies characterizes an exothermic process, also the calculated adsorption energy (−0.42 eV) for CO in C-down is more than that in O-down (−0.12 eV). Therefore, we limited static the external electric field effect to the interaction of CO at the aluminum site with C-down.

Field effect on CO adsorption

The total energy (E_T) and adsorption energies for the optimized structure of CO/AlNNT complex at the aluminum site with C-down at various applied parallel and transverse electric field strengths are summarized in Table 1. The adsorption energies obtained from these calculations at different applied parallel electric field strengths with respect to the corresponding values at zero fields (E_X=E_Y=0) indicates that ,with increasing parallel electric field intensity, the E_T and adsorption energy values increase. The adsorption energy values for the applied transverse electric field show a significant reverse trend, increasing as transverse electric field intensity increased. The calculated adsorption energies show that the CO molecule is bound more tightly as the parallel electric field increases, whereas the adsorption energy value for the applied transverse electric field is decreased gradually from −0.42 eV at zero field strength (E_Y=0) to −0.40 eV at a field strength of 140×10^{-4} a.u (E_Y=140). Therefore, the adsorption energy of the CO molecule for the applied parallel electric field (E_X) from zero field strength to 140×10^{-4}a.u. increases by 90 %, and the adsorption energy of the CO for the applied transverse electric field (E_Y) from zero field strength to 140×10^{-4}a.u. decreases by 5 %. Moreover, the values of $R_{Al\text{-}C}$ in the complex were decreased slightly by the external electric field. The calculated adsorption energies of the complex indicated that CO can be adsorbed significantly on the AlNNT by external parallel electric field (E_X) and the CO adsorption on the AlNNT is

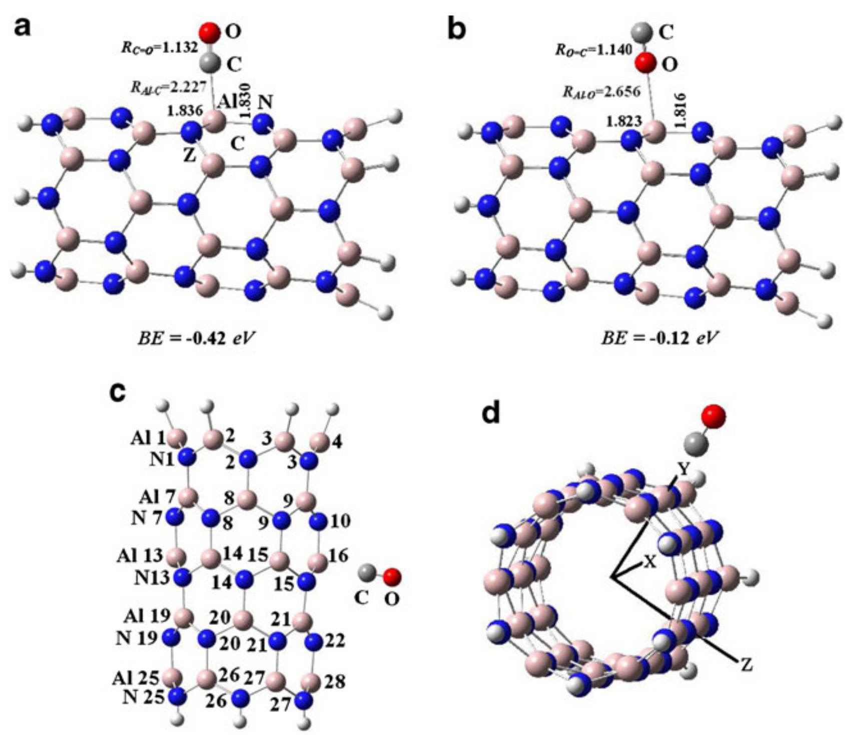

Fig. 1 Two-dimensional (2D) views and adsorption configurations of carbon monoxide (CO; **a** C-down, **b** O-down) on (6,0) zigzag aluminum nitride nanotubes (AlNNT). **c** 2D views of CO/AlNNT complex. **d** Three-dimensional (3D) views of the complex

Table 1 Optimized properties of the carbon monoxide/aluminum nitride nanotubes (CO/AlNNT) complex at different applied parallel and transverse electric field strengths

Property	CO /AlNNT complex								
	X					Y			
	0	35	70	100	140	35	70	100	140
E_T CO /keV	−3.08332	−3.08332	−3.08332	−3.08332	−3.08332	−3.08332	−3.08332	−3.08332	−3.08332
E_T AlNNT/keV	−242.88755	−242.88798	−242.88875	−242.88969	−242.89136	−242.88772	−242.88820	−242.88887	−242.89013
E_T Complex/keV	−245.97129	−245. 97178	−245. 97264	−245. 97367	−245. 97548	−245.97144	−245. 97192	−245. 97259	−245.97385
Adsorption energy (E_{ads}) /eV	−0.42	−0.48	−0.57	−0.66	−0.80	−0.40	−0.40	−0.40	−0.40
energy gaps /eV	4.16	4.02	3.40	2.75	1.75	3.98	3.73	3.50	3.17
$Q_T(e)$	0.173	0.175	0.177	0.179	0.181	0.172	0.170	0.169	0.165
$R_{Al\text{-}C}$	2.227	2.226	2.222	2.219	2.214	2.227	2.227	2.227	2.225
D_M / Debye	12.57	21.15	30.58	38.94	50.35	15.22	21.24	27.58	36.82
Diameter (Al-tip) /Å	6.35	6.35	6.41	6.50	6.64	6.35	6.42	6.52	6.68
Diameter (N-tip) /Å	6.43	6.45	6.48	6.48	6.51	6.43	6.43	6.46	6.53
Length of tube/Å	10.66	10.64	10.61	10.59	10.57	10.64	10.63	10.61	10.59

sensitive to the strength of the electric field applied to the AlNNT surface.

One of the most important characteristics of sensor devices is their recovery time (τ). The strong interactions between the adsorbate and nanotube surfaces shows that desorption of the adsorbate could be difficult and that the nanotube device may suffer from long recovery times. Based on conventional transition state theory, recovery time was calculated as follows:

$$\tau = \nu_0^{-1} \exp(-E_{ads}/kT) \tag{3}$$

Where k is the Boltzmann's constant, T is temperature, and ν_0 is the attempt frequency. According to the above equation, an increase in the adsorption energy (E_{ads}) will prolong the recovery time in an exponential path. However, as is shown in Table 1, the adsorption energies of CO in the applied parallel electric field strengths are not large enough to hinder the recovery of the AlNNT and the recovery time may be short according to above equation. Therefore, with this trend, pristine AlNNT can be used as a CO sensor and increasing the parallel electric field effect (E_X) is a suitable method for CO adsorption on AlNNTs.

Field effects on structural parameters

Structural properties, including bond lengths, bond angles, tip diameters, and length of tube for the optimized structure of the CO/AlNNT complex at various applied parallel and transverse electric field strengths with significant changes in parameters are summarized in Table 2 and Supplementary Table S1. The bond lengths obtained at different applied parallel and transverse electric field strengths with respect to the corresponding values at zero fields (E_X=E_Y=0) indicate that the changes in all Al–N, Al–H, C≡O, and N–H bond lengths of the CO/AlNNT complex over the entire range of the applied parallel and transverse electric field strengths are <0.04 Å (Table 2). The most significant change in bond length for the applied parallel electric field was observed for Al7–N1, which increases gradually from 1.815 Å at zero field strength (E_X=0) to 1.848 Å at a field strength of 140×10^{-4} a.u. (E_X=140). In the case of transverse applied electric fields, the most significant change was observed for Al1–N1, which increases gradually from 1.817 Å at zero field strength (E_Y=0) to 1.847 Å at a field strength of 140×10^{-4} a.u. (E_Y= 140). The Al20–N21 and Al19–N19 bonds show a significant reverse trend, increasing with increasing parallel and transverse electric field intensity.

The variations in bond angles for applied parallel and transverse electric field strengths in Table 2 indicate that the maximum deviation of optimized bond angles with respect to the zero electric field (E_X=E_Y=0) at various parallel and transverse electric field strengths are less than 4°. The most significant change in the bond angles for the applied parallel electric field is observed for N9–Al15–N14, which decreases gradually from 118.61° at zero field strength (E_X=0) to 115.20° at a field strength of 140×10^{-4} a.u. (E_X=140). In the case of transverse applied electric fields, the most significant change was observed for N1–Al7–N8, which decreases gradually from 119.21° at zero field strength (E_Y=0) to 115.20° at a field strength of 140×10^{-4} a.u. (E_Y=140). The results shown in Supplementary material and Table 2 show that the variations in the values of bond lengths and bond angles for applied parallel and transverse electric field strengths in the CO/AlNNT complex are negligible. Therefore, nanotubes are resistant to applied parallel and transverse electric field strengths.

Table 2 Differential values of optimized bond lengths (Å) and bond angles (°) of the CO/AlNNT complex at different applied parallel and transverse electric field strengths

Bond length	CO /AlNNT complex									
	X					Y				
	0	35	70	100	140	0	35	70	100	140
Al1-N1	0.000	−0.003	−0.005	−0.007	−0.010	0.000	0.007	0.015	0.021	0.030
Al2-N1	0.000	0.000	0.001	0.002	0.004	0.000	−0.006	−0.012	−0.016	−0.022
Al2-N2	0.000	−0.008	−0.015	−0.020	−0.026	0.000	0.002	0.005	0.007	0.011
Al3-N2	0.000	0.004	0.007	0.010	0.016	0.000	0.000	0.000	0.000	0.000
Al3-N3	0.000	−0.007	−0.015	−0.021	−0.029	0.000	−0.004	−0.007	−0.010	−0.015
Al4-N3	0.000	0.001	0.003	0.005	0.008	0.000	0.006	0.011	0.017	0.025
Al7-N1	0.000	0.007	0.014	0.022	0.033	0.000	0.000	0.001	0.002	0.003
Al8-N2	0.000	0.006	0.012	0.018	0.026	0.000	0.002	0.005	0.008	0.012
Al9-N3	0.000	0.005	0.010	0.014	0.020	0.000	0.001	0.003	0.005	0.007
Al7-N7	0.000	−0.001	−0.002	−0.003	−0.003	0.000	−0.006	−0.012	−0.017	−0.024
Al7-N8	0.000	−0.005	−0.010	−0.014	−0.019	0.000	−0.003	0.011	0.017	0.024
Al8-N8	0.000	0.002	0.005	0.008	0.011	0.000	−0.003	−0.005	−0.007	−0.009
Al8-N9	0.000	−0.008	−0.015	−0.021	−0.029	0.000	0.001	0.001	0.002	0.004
Al9-N9	0.000	0.002	0.004	0.005	0.007	0.000	0.004	0.009	0.013	0.020
Al9-N10	0.000	−0.005	−0.009	−0.013	−0.017	0.000	−0.005	−0.010	−0.015	−0.021
Al13-N7	0.000	−0.002	0.014	0.022	0.032	0.000	0.000	0.000	0.000	0.000
Al14-N8	0.000	0.007	0.014	0.020	0.029	0.000	0.002	0.003	0.004	0.006
Al15-N9	0.000	0.005	0.011	0.016	0.024	0.000	0.002	0.004	0.006	0.009
Al16-N10	0.000	0.006	0.013	0.020	0.030	0.000	0.000	−0.020	−0.001	−0.001
Al13-N13	0.000	−0.002	−0.004	−0.005	−0.007	0.000	0.006	0.013	0.019	0.027
Al14-N13	0.000	0.001	0.002	0.003	0.006	0.000	−0.005	−0.010	−0.013	−0.018
Al14-N14	0.000	−0.007	−0.014	−0.020	−0.027	0.000	0.003	0.007	0.011	0.016
Al15-N14	0.000	0.003	0.006	0.009	0.012	0.000	0.002	0.003	0.005	0.008
Al15-N15	0.000	−0.007	−0.015	−0.021	−0.028	0.000	−0.002	−0.004	−0.005	−0.007
Al16-N15	0.000	0.002	0.003	0.005	0.008	0.000	0.005	0.011	0.016	0.024
Al19-N13	0.000	0.006	0.013	0.019	0.028	0.000	0.000	0.001	0.002	0.002
Al20-N14	0.000	0.006	0.012	0.017	0.024	0.000	0.002	0.003	0.004	0.006
Al21-N15	0.000	0.004	0.009	0.013	0.020	0.000	0.001	0.001	0.002	0.004
Al19-N19	0.000	−0.002	−0.002	−0.003	−0.003	0.000	−0.007	−0.013	−0.018	−0.025
Al19-N20	0.000	−0.005	−0.010	−0.013	−0.017	0.000	0.006	0.013	0.019	0.027
Al20-N20	0.000	0.003	0.006	0.008	0.012	0.000	−0.001	−0.003	−0.003	−0.005
Al20-N21	0.000	−0.008	−0.015	−0.022	−0.030	0.000	0.001	0.003	0.005	0.007
Al21-N21	0.000	0.001	0.002	0.003	0.007	0.000	0.005	0.010	0.015	0.022
Al21-N22	0.000	−0.006	−0.012	−0.016	−0.022	0.000	−0.005	−0.010	−0.013	−0.018
Al25-N19	0.000	0.005	0.010	0.016	0.022	0.000	0.000	0.000	0.001	0.001
Al26-N20	0.000	0.005	0.010	0.015	0.021	0.000	0.000	0.001	0.002	0.003
Al27-N21	0.000	0.005	0.010	0.015	0.021	0.000	0.001	0.002	0.002	0.004
Al28-N22	0.000	0.005	0.010	0.015	0.023	0.000	0.000	0.001	0.002	0.002
Al25-N25	0.000	−0.001	−0.001	−0.001	−0.001	0.000	0.007	0.014	0.020	0.030
Al26-N25	0.000	0.003	0.005	0.008	0.013	0.000	−0.005	−0.009	−0.012	−0.017
Al26-N26	0.000	−0.006	−0.012	−0.016	−0.023	0.000	0.005	0.011	0.016	0.023
Al27-N26	0.000	0.004	0.008	0.012	0.017	0.000	0.003	0.006	0.009	0.013
Al27-N27	0.000	−0.007	−0.014	−0.019	−0.026	0.000	−0.001	−0.003	−0.004	−0.005
Al28-N27	0.000	−0.001	−0.001	−0.001	0.000	0.000	0.007	0.014	0.021	0.031
Average Al-N	0.000	0.000	0.001	0.002	0.004	0.000	0.001	0.002	0.003	0.005

Table 2 (continued)

Bond length	CO /AlNNT complex									
	X					Y				
	0	35	70	100	140	0	35	70	100	140
C≡O	0.000	−0.002	−0.004	−0.005	−0.007	0.000	0.000	0.000	0.001	0.001
Al-H	0.000	0.010	0.010	0.020	0.030	0.000	0.000	0.010	0.010	0.020
N-H	0.000	0.000	0.000	0.000	0.000	0.000	0.000	0.000	0.000	0.000
Bond angles										
N1-Al7-N8	0.000	−0.060	−0.110	−0.140	−0.160	0.000	−0.730	−1.520	−2.230	−3.220
N2-Al8-N9	0.000	0.370	0.790	1.150	1.610	0.000	−0.230	−0.550	−0.870	−1.370
N7-Al13-N13	0.000	−0.380	−0.790	−1.150	−1.640	0.000	−0.580	−1.150	−1.630	−2.300
N8-Al14-N14	0.000	0.100	0.220	0.340	0.510	0.000	−0.400	−0.820	−1.200	−1.740
Al14-N14-Al20	0.000	0.010	0.060	0.120	0.240	0.000	−0.520	−1.040	−1.500	−2.140
N9-Al15-N14	0.000	−0.830	−1.680	−2.410	−3.410	0.000	−0.200	−0.420	−0.620	−0.910
N10-Al16-N15	0.000	−0.620	−1.280	−1.890	−2.790	0.000	−0.440	−0.880	−1.270	−1.860
N20-Al20-N21	0.000	0.580	1.160	1.680	2.380	0.000	0.400	0.750	1.000	1.290
N21-Al27-N27	0.000	0.040	0.080	0.110	0.160	0.000	0.520	1.020	1.440	2.000

The length of the CO/AlNNT complex is an important parameter characterizing the structural response to the applied parallel and transverse electric field in the nanoelectronic circuit. The distance between the Al2 and Al26 atoms of the complex (see Fig. 1c) is considered as the length (l) of the complex. The calculated lengths and tip diameters of the complex at various parallel and transverse electric field strengths with respect to the zero field (E_X= E_Y=0) are presented in Table 1. The results indicate that the length of the complex does not change significantly with any increasing electric field strengths (< 0.84 %). The length resistance of the complex against the external electric field can be considered as an advantage of the complex in molecular scale devices. Likewise, the values of tip diameters in the complex were increased slightly by the external electric field.

Field effects on electronic properties of the CO/AlNNT complex

Densities of states

The influence of the external electric field on the electronic properties of the complex was studied. The total densities of states (DOS) of the complex at various applied parallel and transverse electric field strengths are shown in Fig. 2. As it is shown in Fig. 2 and Table 1, the energy gap obtained from these calculations indicates that, with increasing parallel and transverse electric field intensity, the energy gap values decrease. The energy gap value for the applied parallel electric field is decreased gradually from 4.16 eV at zero field strength (E_X=0) to 1.75 eV at a field strength of 140× 10^{-4} a.u. (E_X=140) and the value for the applied transverse electric field also decrease gradually from 4.16 eV at zero field strength (E_Y=0) to 3.17 eV at a field strength of 140× 10^{-4} a.u. (E_Y=140). The total densities of states (TDOS) of the complex show significant changes due to the external electric field in the gap regions of the TDOS plots. In

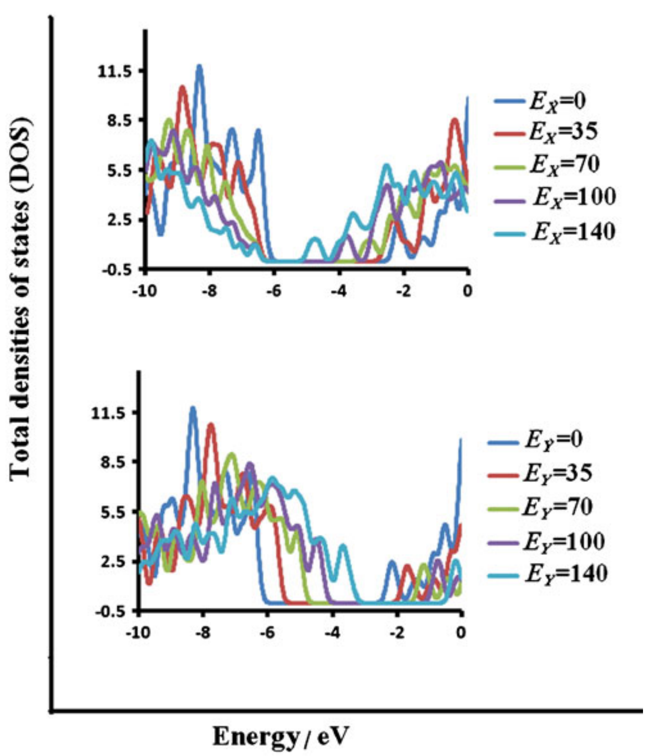

Fig. 2 Total densities of states (TDOS) for the CO/AlNNT complex at different applied parallel and transverse electric field strengths

comparison with zero field strength, the energy gaps of the complex due to external electric field were reduced while their electrical conductance was increased. These results also show that the applied parallel electric field has more influence on the energy gap of the complex than the applied transverse electric field due to the stronger interaction of the CO molecule with the AlNNT. This trend is in agreement with the changes seen in the adsorption energies of the complex within the complex, with the applied parallel electric field having a stronger effect than the applied transverse electric field on the adsorption energy of the complex (Table 1).

Molecular orbital

To better understand the electric response and electrical transport in CO/AlNNT complex, we studied the electronic energies of the complex at different applied parallel and transverse electric field strengths. The electric response and electrical transport depend on all the molecular orbital (MO) energy spacings between the occupied and virtual MOs. The highest occupied molecular orbital (HOMO) and lowest unoccupied molecular orbital (LUMO) for the complex as functions of the different applied parallel, E_X, and perpendicular, E_Y, electric field strengths are plotted in Fig. 3. The HOMO and LUMO are both stabilized more in the parallel case than in the perpendicular case. The HOMO and LUMO values in the applied parallel electric field increased gradually from −6.36 and −2.20 eV at zero field strength (E_X=0) to −6.61 and −4.86 eV at a field strength of 140×10^{-4}a.u. (E_X=140). On the other hand, the HOMO and LUMO values for the applied perpendicular electric field decreased gradually from −6.36 and −2.20 eV at zero field strength (E_Y=0) to −3.43 and −0.26 eV at a field strength of 140×10^{-4}a.u. (E_Y=140) (see Table 3). Therefore, the electronic energies study of the complex show the strong interaction of the CO molecule on the AlNNT in the applied parallel electric field. Also, adsorption of the CO molecule on the AlNNT in the applied parallel electric field decreases the energy gap of the pristine AlNNT significantly, and increases the

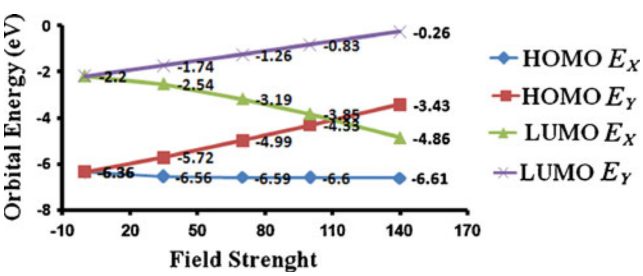

Fig. 3 highest occupied molecular orbital (HOMO) and lowest unoccupied molecular orbital (LUMO) for the CO/AlNNT complex at different applied parallel and transverse electric field strengths

electrical conductance. The electric conductivity of the complex was calculated as follows [18]:

$$\sigma \propto \exp\left(\frac{-E_g}{2kT}\right) \tag{4}$$

Where σ is the electric conductivity of the complex and k is the Boltzmann's constant. According to the above equation, a smaller energy gap (E_g) at a particular temperature leads to the larger electric conductivity. However, in the complex, E_g decreases from 4.16 eV at zero field strength (E_X=0) to 1.75 eV at a field strength of 140×10^{-4}a.u. (E_X=140) in the applied parallel electric field (see Table 1). The significant change in energy gap value shows the high sensitivity of the electronic properties of AlNNT upon adsorption of the CO molecule.

LUMO energy of the complex at different electric field strengths

One of the most important factors in HOMO/LUMO interactions is the energy difference between the HOMO of the CO molecule and LUMO of the nanotube. Our FMO analysis indicates that the HOMO energy of the CO molecule is −10.11 eV, and the LUMO energies for the complex at different applied parallel and transverse electric field strengths are shown in Table 3, suggesting that the large value of adsorption energy (E_{ad}=−0.80 eV) for the complex at a field strength of 140×10^{-4}a.u. (E_X=140) may come from its smaller LUMO energy level (−4.86 eV). Therefore, due to the decreasing energy level of the LUMO of the complex with increasing applied parallel electric field strengths, its nanotube has a much stronger interaction with the CO molecule. The increase in LUMO energy of the complex with increasing applied transverse electric field strengths suggests that the relatively small adsorption energy of the complex may come from its higher LUMO energy level. An interesting conclusion that can be drawn from these investigations is that this factor can affect values of energy adsorption depending on external electric field strengths.

Dipole moment

When a nanotube is placed in an external electric field, its atomic charge distribution is easily changed as are the centers of the positive and negative charge of the nanotube due to the redistribution of atomic charges. Consequently, there is a polarization of the nanotube and an induced electric dipole moment (D_M). As is obvious from Table 1, the values of the induced electric D_M vector obtained from these calculations increases linearly with an upward trend in the applied external electric field strengths. Thus, the

Table 3 Quantum molecular descriptors of the CO/AlNNT complex at different applied parallel and transverse electric field strengths. *I* Ionization potential, *A* electron affinity, η global hardness, *S* softness, μ chemical potential, ω electrophilicity

Property	CO /AlNNT complex									
	X					Y				
	0	35	70	100	140	0	35	70	100	140
E_{HOMO} /eV	−6.36	−6.56	−6.59	−6.60	−6.61	−6.36	−5.72	−4.99	−4.33	−3.43
E_{LUMO} /eV	−2.20	−2.54	−3.19	−3.85	−4.86	−2.20	−1.74	−1.26	−0.83	−0.26
[E_{LUMO} -E_{HOMO}] /eV	4.16	4.02	3.40	2.75	1.75	4.16	3.98	3.73	3.50	3.17
[I=− E_{HOMO}] /eV	6.36	6.65	6.59	6.60	6.61	6.36	5.72	4.99	4.33	3.43
[A=− E_{LUMO}] /eV	2.20	2.54	3.19	3.85	4.86	2.20	1.74	1.26	0.83	0.26
[η=(I − A)/2] /eV	2.08	2.01	1.70	1.38	0.88	2.08	1.99	1.87	1.75	1.59
[μ=− (I+A)/2] /eV	−4.28	−4.55	−4.89	−5.23	−5.74	−4.28	−3.73	−3.13	−2.58	−1.85
[S=1/2η] /eV^{-1}	0.24	0.25	0.29	0.36	0.57	0.24	0.25	0.27	0.29	0.31
[ω=μ^2/2 η] /eV	4.40	5.15	7.03	9.91	18.72	4.40	3.50	2.62	1.90	1.08

electric D_M of a nanotube is an important property that characterizes its electronic and geometrical structure. The size and components of the electric D_M (in Debye) for the complex at various applied parallel and transverse electric field strengths are shown in Fig. 4. $D_{M\ Tot}$ variations for the applied parallel electric field increased gradually from 12.57 Debye at zero field strength (E_X=0) to 50.35 Debye at a field strength of 140×10^{-4}a.u. (E_X=140). $D_{M\ Tot}$ variations for the applied transverse electric field also increased gradually from 12.57 Debye at zero field strength (E_Y=0) to 36.82 Debye at a field strength of 140×10^{-4}a.u. (E_Y= 140). These results show that when the complex is exposed to an external electric field, it has a much stronger interaction with the electrodes of the nano-electronic circuit.

Charge density distribution

As discussed above, the electronic charge distribution on atoms of the nanotube changes because of the applied external electric field strengths and, consequently, all charge-related molecular properties became different. Therefore, the study of the electric field-dependent charge distribution that determines molecular behavior directly is important. In order to study the atomic charge distribution as a function of the parallel and transverse electric field strengths (E_X and E_Y), the natural bond orbital charges (NBO) [19] were calculated and are plotted in Fig. 5.

As shown in Fig. 5, the large variations in Al atom charge distributions at different parallel electric field strengths (E_X) are on Al28 and Al7 atoms, which increased and decreased gradually with field strength, respectively. In Fig. 5, a similar trend in atomic charge variations was observed on atoms N24 and N12. For the applied transverse electric field strengths (E_Y), large variations in the Al atom charge distributions were seen on Al30 and Al27 atoms, which increased and decreased gradually with field strength; a similar trend in atomic charge variations was observed on atoms N2 and N14. As is evident from Fig. 5, the atomic charge variations obtained from these calculations increase with any upward trend in the applied external electric field strength. Moreover, separation of the center of the positive and negative electric charges of the CO/AlNNT complex increases with the increase in applied external electric field strength.

Fig. 4 Size of the electric dipole moment (D_M) vector and its components (in Debye) at different applied parallel and transverse electric field strengths

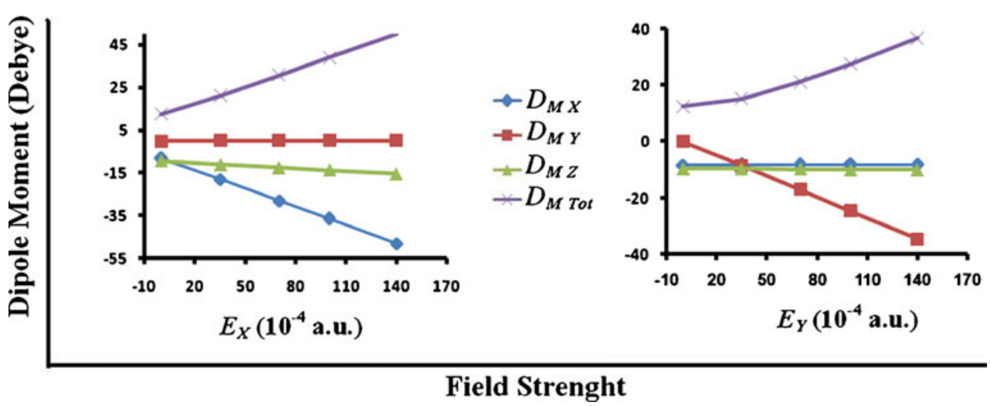

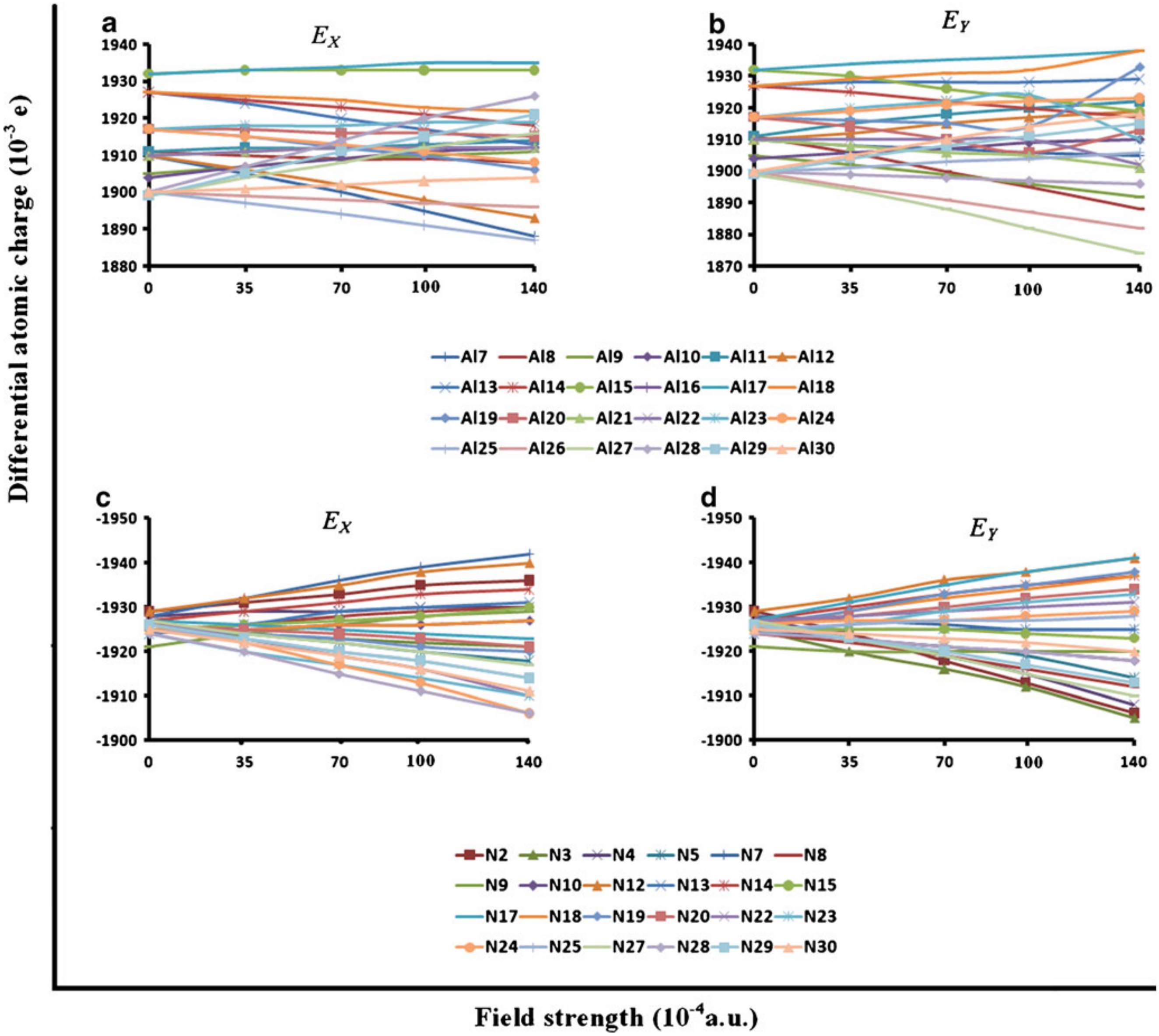

Fig. 5 Natural bond orbital (NBO) charges at different applied parallel and transverse electric field strengths on the Al atoms (**a**, **b**) and N atoms (**c**, **d**) in the CO/AlNNT complex

The charge distribution can be explained by molecular electrostatic potential (MEP) calculations. The MEP is the potential generated by the charge distribution of the nanotube, which is defined for each atomic site as follows:

$$V(r) = \sum\nolimits_{A}(Z_A/R_A - r) - \int \rho\left(r'\right)dr' \Big/ \left|r' - r\right| \qquad (5)$$

Where Z_A is the charge on nucleus A, located at R_A. The V (r) depends on whether the effects of the nuclei or the electrons are dominant at any point. We computed the MEP surfaces for the CO/AlNNT complex in the different applied parallel (E_X) and perpendicular (E_Y) electric field strengths. The MEP has been used to explore the chemical properties of several materials [20, 21]. As shown by the MEP plots in Fig. 6, in the pristine (6,0) zigzag AlNNT, the aluminum atoms are positively charged (blue) while the N atoms are relatively negatively charged (yellow or red) in Al–N bonds of the pristine surface. This indicates that some charge is transferred from the Al atoms to the N atoms, resulting in an ionic bonding in AlNNT surface. On the other hand, as shown in Fig. 6a, the C atom of the CO molecule is more negative (red) than its O atom; therefore, it is expected that the electron carbon atom of CO should interact with the electron Al atom of the pristine surface. In Fig. 6c, the CO-attached (6,0) AlNNT complex at zero field strength (E_X, E_Y=0) shows that, after the adsorption process, the CO fragment is more positive (blue) confirming a charge transfer from CO to the pristine

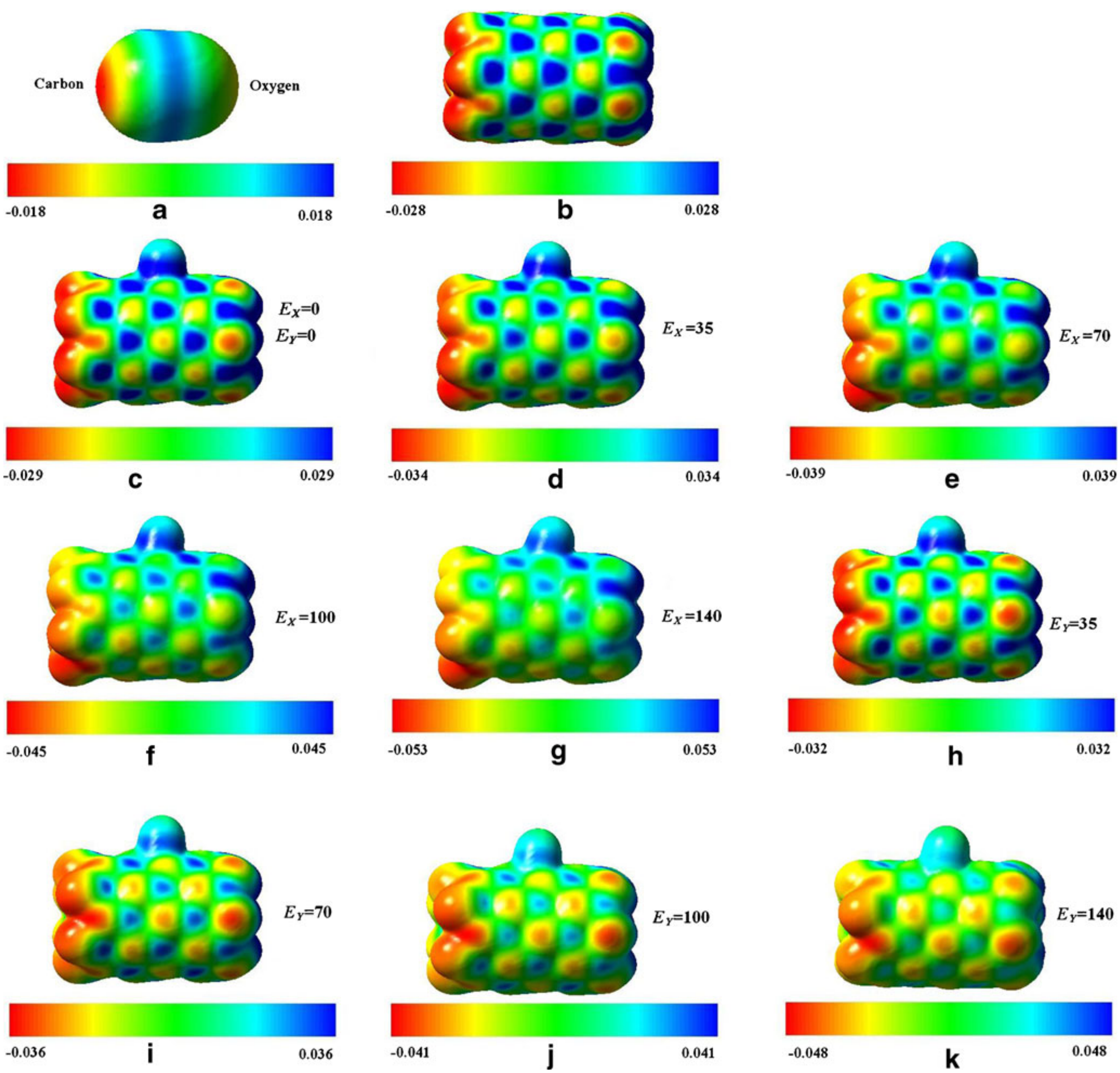

Fig. 6 Computed B3LYP/6-31G* electrostatic potentials on the molecular surfaces of (**a**) an isolated CO molecule (**b**) a pristine (6,0) AlNNT, and (**c**–**k**) the CO/AlNNT complex at different applied parallel and transverse electric field strengths. The surfaces are defined by the 0.0004 electrons/b3 contour of the electronic density. Color ranges are in a.u.

surface due to an interaction. As shown in Fig. 6, with increase in the applied parallel electric field strengths (E_X), the charge transfer from CO to the AlNNT increases gradually, whereas with an increase in the applied transverse electric field strengths (E_Y), the charge transfer from CO to the AlNNT decreases gradually (see CO fragment colors).

Charge transfer from CO molecule to AlNNT

The variations in electronic properties of the complex in CO adsorption show a charge transfer from the CO molecule to the nanotube. The amount of charge transfer between the CO molecule and the nanotube (Q_T) is given in Table 1. Positive values of Q_T indicate that the CO molecule acts as an electron donor, while a negative value of Q_T indicates that the CO molecule act as an electron acceptor. The charge value transferred from the CO molecule to the AlNNT in the applied parallel electric field is increased gradually from 0.173e at zero field strength (E_X=0) to 0.181e at a field strength of 140×10^{-4}a.u. (E_X=140) and its value for the applied transverse electric field is decreased gradually from 0.173e at zero field strength (E_Y=0) to 0.165e at a field strength of 140×10^{-4} a.u. The results confirm the high adsorption energy and sensitivity of the AlNNT towards the CO molecule in the applied parallel electric field.

Quantum molecular descriptors

The quantum molecular descriptors for the CO/AlNNT complex in the different applied parallel (E_X) and perpendicular (E_Y) electric field strengths are summarized in Table 3. We observe that with any increase in the applied external electric field strengths, the energy gap ($E_{LUMO}-E_{HOMO}$) of the complex decreased. This lowering of energy gap in the complex may be able to increase the reactivity of the complex. The results in Table 3 indicate that the ionization potential (I) and electron affinity (A) of the complex for the applied parallel electric field is increased gradually from 6.36 eV to 2.20 eV at zero field strength (E_X=0) to 6.61 and 4.86 eV at a field strength of 140×10^{-4} a.u. (E_X=140), whereas the ionization potential (I) and electron affinity (A) of the complex for the applied transverse electric field decreases gradually from 6.36 eV to 2.20 eV at zero field strength (E_Y=0) to 3.43 and 0.26 eV at a field strength of 140×10^{-4} a.u. (E_Y=140). The chemical potential (μ) with the increase in applied parallel electric field strengths is increased gradually, whereas with increase of the applied transverse electric field, strengths decrease gradually. The electrophilicity index (ω) is a measure of the electrophilic power of a molecule. The electrophilicity of the complex with increased applied parallel electric field strengths is increased strongly, whereas with any increase in the applied transverse electric field strengths are decreased gradually. These trends are in agreement with changes in the adsorption energies of the complex, explaining why the adsorption energy values of the complex show a significant reverse trend with increasing applied transverse electric field (E_Y). The global hardness (η) of the complex at different external electric field strengths decreased and, consequently, the global softness (S) of the complex increased. The decrease in global hardness and the energy gap of the complex is due to the external electric field strength, and, consequently, the stability of the complex is lowered and its reactivity increased. This increasing in the ionization potential (I) , electron affinity (A), chemical potential (μ), electrophilicity (ω), and HOMO and LUMO in CO adsorption with increase of the applied parallel electric field strengths may be able to increase the reactivity of the complex, and show charge transfer taking place between the CO and pristine AlNNT sidewalls.

Conclusions

We studied the adsorption of the CO molecule on the (6,0) zigzag AlNNT, as well as structural and electronic properties including bond lengths, bond angles, length of tube, tip diameters, dipole moment variations, energy gaps, energies, atomic charges, molecular orbital energies, adsorption energy, density of states, and quantum molecular descriptors. The study was carried out at different applied parallel and transverse electric field strengths by means of DFT calculations. We compared all the adsorption energies of CO interacting with all possible sites of adsorption on the nanotube walls in several structural configurations. The calculated adsorption energy for CO in the C-down configuration is higher than that in O-down, and the aluminum site was the most stable configuration. The adsorption energies obtained from these calculations at different applied parallel electric field strengths with respect to the corresponding values at zero fields indicates that, with any increase in parallel electric field intensity, total energy and adsorption energy values increase. So CO could be absorbed significantly on AlNNT, especially at higher parallel field strengths, whereas the adsorption energy values for the applied transverse electric field show a significant reverse trend. Therefore, the parallel electric field effect is a suitable method for adsorption, storage, and fabrication of CO sensors. The length and tip diameters of the complex do not change significantly with any increase in the electric field strength, indicating that the complex is stable over the entire range of the applied electrical field strength. The dipole moment variations of the complex increase linearly with increases in the applied external electric field strengths. We also showed that when the complex is exposed to an external electric field, it has a much stronger interaction with the electrodes of the nanoelectronic circuit. Analysis of DOS, MO energies, LUMO energy, charge transfer of the CO molecule, NBO charges, and quantum molecular descriptors of the complex show that with increasing applied parallel electric field strengths, the nanotube can detect the CO molecule significantly and thus can be used as CO storage.

References

1. Beheshtian J, Bagheri Z, Kamfiroozi M, Ahmadi A (2012) Struct Chem 23:653–657
2. Wang R, Zhang D, Sun W, Han Z, Liu C (2007) J Mol Struct (THEOCHEM) 806:93–97
3. Zhao JX, Dinga YH (2008) Mater Chem Phys 110:411–416
4. Beheshtian J, Kamfiroozi M, Bagheri Z, Ahmadi A (2011) Physica E 44:546–549
5. Tondare VN, Balasubramanian C, Shende SV, Joag DS, Godbole VP, Bhoraskar SV, Bhadbhade M (2002) Appl Phys Lett 80:4813–4815
6. Balasubramanian C, Bellucci S, Castrucci P, De Crescenzi M, Bhoraskar SV (2004) Chem Phys Lett 383:188–191
7. Stan G, Ciobanu C, Thayer T, Wang G, Creighton J, Purushotham K, Bendersky L, Cook R (2009) Nanotechnology 20:35706–357014

8. Ruterana P, Albrecht M, Neugebauer J (2003) Nitride semiconductors: handbook on materials and devices. Wiley, New York
9. Khoo KH, Mazzoni MSC, Louie SG (2004) Phys Rev B 69:201401(R)
10. Guo GY, Ishibashi S, Tamura T, Terakura K (2007) Phys Rev B 75:245403
11. Attaccalite C, Wirtz L, Marini A, Rubio A (2007) Phys Status Solidi B 244:4288–4292
12. Chattaraj PK, Sarkar U, Roy DR (2006) Chem Rev 106:2065–2091
13. Hazarika KK, Baruah NC, Deka RC (2009) Struct Chem 20:1079–1085
14. Parr RG, Szentpaly L, Liu S (1999) J Am Chem Soc 121:1922–1924
15. Baierle RJ, Schmidt TM, Fazzio A (2007) Solid State Commun 142:49–53
16. Sabzyan H, Farmanzadeh D (2007) J Comput Chem 28:923–931
17. Schmidt M et al (1993) J Comput Chem 14:1347–1363
18. Li SS (2006) Semiconductor physical electronics, 2nd edn. Springer, New York
19. Reed AE, Weinstock RB, Weinhold F (1985) J Chem Phys 83:735–746
20. Politzer P, Lane P, Murray JS, Concha MC (2005) J Mol Model 11(1):1
21. Peralta-Inga Z, Lane P, Murray JS, Boyd S, Grice ME, O’Connor CJ, Politzer P (2003) Nano Lett 3(1):21–28